JOURNAL OF PROPULSION AND POWER
Vol. 10, No. 1, Jan.–Feb. 1994

Internal Reversing Flow in a Tailpipe Offtake Configuration for ASTOVL Aircraft

Jack G. McArdle* and Barbara S. Esker†
NASA Lewis Research Center, Cleveland, Ohio 44135
and
James A. Rhodes‡
McDonnell-Douglas Aerospace Company, St. Louis, Missouri 63166

A generic one-third scale model of a tailpipe offtake system for an advanced short takeoff vertical landing (ASTOVL) aircraft was tested with unheated air at tailpipe-to-ambient pressure ratios up to 5. The model consisted of a tailpipe with twin elbows, offtake ducts, and offtake flow control nozzles, plus a small ventral nozzle and a blind flange to simulate a blocked cruise nozzle. The offtake duct-to-tailpipe diameter ratio was 0.74. The offtake openings in the tailpipe had sharp edges. The offtake flow turned through a total angle of 177 deg relative to the tailpipe inlet axis. The flow split was 45% to each offtake and 10% to the ventral nozzle. The total pressure loss through the offtakes was as high as 15.5%. All test results are shown as graphs, contour plots, and wall pressure distributions. The complex flow patterns in the tailpipe and elbows at the offtake openings are described with traversing flow angle probe and paint streak flow visualization data. A computational fluid dynamics (CFD) analysis of the same configuration was made. Comparison of the experimental and preliminary CFD results were reported previously.

Nomenclature

A = area, in.^{2}
D = diameter, in.
M = Mach number, for air, $\sqrt{5[(P/p_w)^{0.2857} - 1]}$
P = total pressure, psia
PR = pressure ratio relative to ambient pressure
p = static pressure, psia
q = dynamic pressure, psi
R = radius of curvature at elbow centerline, in.
w = measured airflow rate, pps
δ = ratio of pressure to standard-day pressure, 14.696 psia
θ = ratio of temperature to standard-day temperature, 518.7°R

Subscripts
d = offtake duct
n = offtake nozzle
tp = tailpipe
v = ventral nozzle
w = wall static pressure

Introduction

SEVERAL proposed powered lift concepts for advanced short takeoff vertical landing (ASTOVL) aircraft are based on blocking the cruise exhaust nozzle and redirecting engine gas forward to lift thrusters during landing, short takeoff, or hover flight. In addition, a small ventral nozzle might be needed to balance vertical forces or to provide pitch trim and control. A typical concept is sketched in Fig. 1a. The lift thrusters could be ejectors, burners, lift nozzles, or gas-driven lift fans. In every case, the available lift is directly reduced by the pressure loss in the tailpipe offtakes and ducts leading to the thrusters. The fluid dynamic mechanisms causing pressure loss are known to be very complex, and large losses in some configurations have been reported.[1]

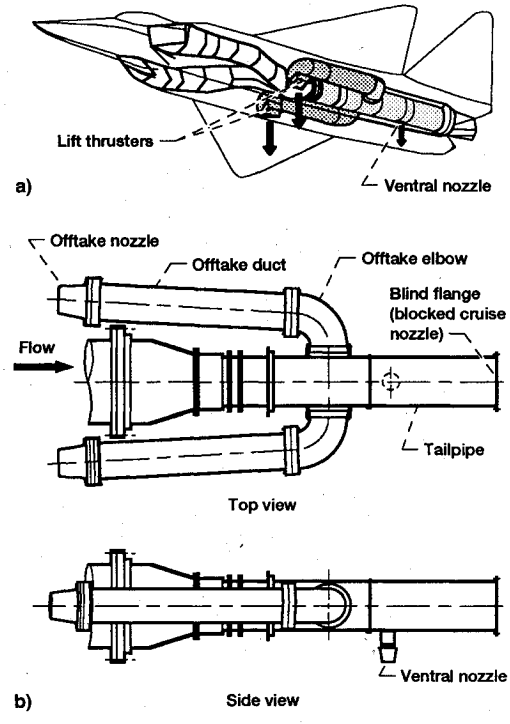

Fig. 1 ASTOVL Powered lift system using engine exhaust gas: a) ASTOVL aircraft and b) model tested.

Presented as Paper 92-3790 at the AIAA/SAE/ASME/ASEE 28th Joint Propulsion Conference, Nashville, TN, July 6–8, 1992; received Aug. 31, 1992; revision received June 7, 1993; accepted for publication June 15, 1993.

*Senior Research Engineer, Hypersonics and Engine Integration Branch, Propulsion Systems Division.
†Aerospace Engineer, Hypersonics and Engine Integration Branch, Propulsion Systems Division. Member AIAA.
‡Lead Engineer, Propulsion and Thermodynamics Department. Senior Member AIAA.

One of the ASTOVL technology goals is to determine if the flow behavior in various exhaust configurations can be modeled and predicted successfully with computational fluid dynamics (CFD) programs. To this end, the internal flow patterns and performance of a generic tailpipe, closed at the aft end and having a large ventral nozzle, were computed with the PARC3D code.[2] The results[3,4] compared very favorably with experimental data from the same configuration. For instance, the predicted ventral nozzle discharge and thrust coefficients were only about 1 percentage point greater than the measured values. In addition, the internal flow patterns shown by experimental paint streaks and CFD flow visualization images were remarkably similar. This same computational-plus-experimental approach has now been extended to a one-third scale generic tailpipe offtake configuration. The model, sketched in Fig. 1b, was designed for ease in generating a grid for the CFD analysis. It retained all the essential features of an ASTOVL aircraft with this type of powered lift system, except for thrusters. The model consisted of a tailpipe with twin elbows, offtake ducts, and offtake flow-control nozzles, plus a small ventral nozzle and a blind flange to simulate a blocked cruise nozzle. All ducts were round in cross section. The offtake duct-to-tailpipe diameter ratio was 0.74. The offtake openings in the tailpipe had unrounded edges. Offtake flows were turned through 177 deg relative to the tailpipe inlet axis. The total tailpipe flow was split nominally 45% to each offtake and 10% to the ventral nozzle. The model was tested with unheated air over a range of tailpipe-to-ambient pressure ratios up to 5. Performance criteria, such as system pressure loss and duct Mach number, are reported over the range of measured pressure ratios for two preliminary (smaller) nozzle sizes as well as for the final size. Details of performance, such as wall pressures, flow patterns, duct total-pressure contours, and elbow inflow direction and velocity are shown for the final nozzle size at a tailpipe pressure ratio of 4.5. Thrust produced by the model was not measured.

A CFD analysis of the same configuration was made using the McDonnell Aerospace computational grid system (MACGS) and Navier-Stokes time dependent (NASTD) codes, and the PARC3D code. Comparison of the experimental and preliminary CFD results has been reported.[5] Additional CFD analysis is being done to improve modeling technique.

Apparatus

A schematic diagram of the experimental model is shown in Fig. 2. An inlet reducer section contained flow straighteners, a screen, and a boundary-layer trip to ensure uniform flow with a turbulent boundary layer into the model tailpipe. The model tailpipe diameter was 13.5 in., which is approximately one-third the diameter of modern military engines. The aft end of the tailpipe was blocked with a blind flange to simulate a closed cruise nozzle.

Attached to the tailpipe were two identical circular cross section offtakes located 180-deg apart. The offtake duct and tailpipe centerlines were all located in the same horizontal plane. The offtakes intersected the tailpipe perpendicularly and had unrounded edges at the intersections. Each offtake consisted of a 10-in.-diam elbow and straight duct and a nozzle. The elbow had a 10-in. centerline radius of curvature and an 87-deg arc. The straight ducts, attached to the elbows, thereby were canted 3 deg away from the tailpipe to avoid interference with facility flanges. At the end of the straight ducts were American Society of Mechanical Engineers (ASME) long-radius flow-measuring nozzles[6] to provide back pressure for the system and to meter the offtake flow.

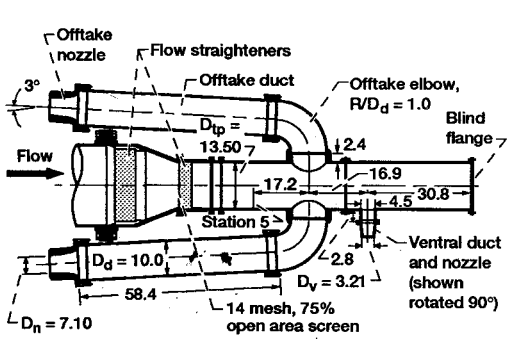

Fig. 2 Top view of tailpipe offtake duct model. (All dimensions given in inches.)

A small, ventral duct was located in the vertical plane aft of the offtakes. The duct was 4.5 in. in diameter and had unrounded edges at the tailpipe intersection. The ventral nozzle had a 15-deg half-angle conical shape.

The experimental model was tested on the NASA Lewis Powered Lift Facility with unheated pressurized air from the central air system.

Instrumentation and Data

Model Instrumentation

Philosophy

Instrumentation was located throughout the model to provide data for quantitative comparison with CFD results. Accordingly, wall pressure taps were installed at many locations along the flowpath. Freestream total pressure rakes with tubes located on centers of equal area were located at several stations. Additional total pressure tubes were located in the boundary layer. Rakes were always the same in each of the offtake ducts in order to keep equal flow in both sides. Except for a flow angle probe for traverses, no rakes were placed at an offtake entrance lest a rake impede or alter the offtake inflow. Ambient pressure, inlet air total temperature, and an independent total airflow measurement (previously found to be accurate within $\pm 0.5\%$) were obtained from existing facility equipment.

Pressure and Temperature Instrumentation

The model station and instrumentation diagrams are given in Fig. 3. Flow total temperature was assumed to be constant through the model, so stream thermocouples were not used. The model contained up to 248 steady-state pressure measurements on an electronically scanned system, and two wall temperature thermocouples. Pressure transducers, having calculated installed frequency response flat ($\pm 5\%$) to 180 Hz, were used to measure dynamic pressures.

Flow Angle Probe

A flow angle probe with a five-port sensing tip[7] was used to measure stream flow angles, plus stream total pressure and Mach number, at station 5A2. The probe was calibrated in an open jet at Mach numbers of 0.3, 0.5, and 0.8 over ranges of angles greater than encountered in the flow pattern tests.

Data Recording and Processing

Steady-State Data

After airflow in the model had become steady, 20 scans of all the instrumentation were made at the rate of 1 scan/s and recorded by the laboratory central data system. The final computations were batch processed from the averaged data on a mainframe computer.

Total airflow was measured with the facility ASME flow-measuring nozzle, located in the facility air supply piping, using ASME recommended procedures and coefficients. Ventral nozzle flow was computed with isentropic flow equations and necessary measured data, using published discharge coefficients[8] (0.970 for a hard-choked 15-deg conical nozzle). Offtake flow in each side was computed using ASME coefficients[6] and necessary measured data. The final nozzle sizes had a 0.71 throat-to-inlet diameter ratio. The throat Reynolds number was as high as 8.4×10^6.

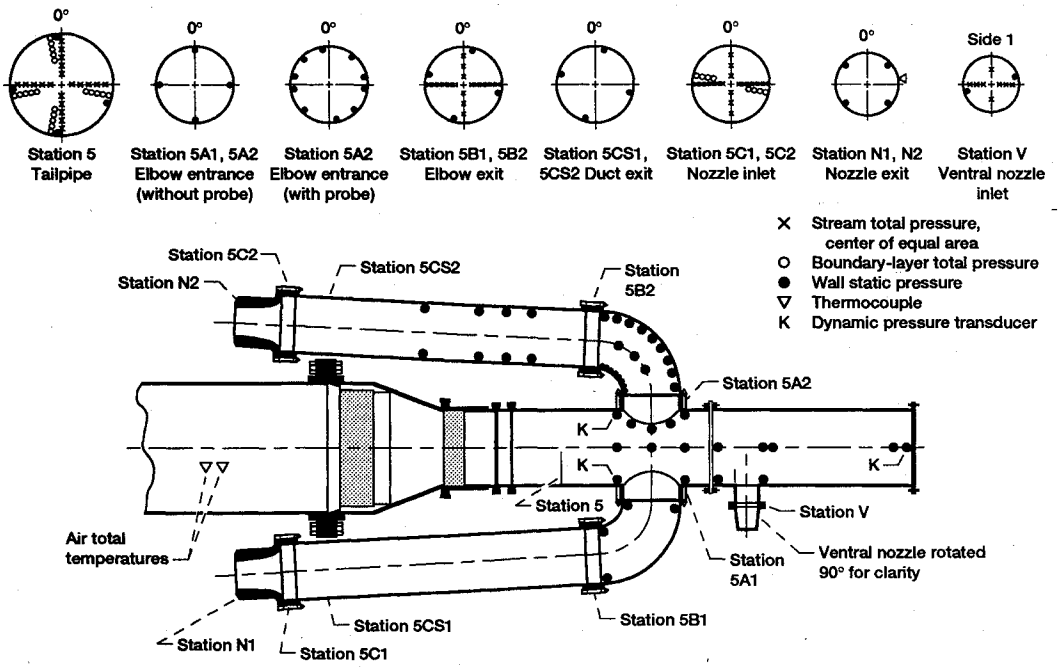

Fig. 3 Station and instrumentation diagrams. Station cross sections drawn looking into flow, with top at 0 deg. 5, 5A, 5B, 5C, 5CS = station numbers (if followed by 1 or 2, refers to a particular offtake side).

Dynamic Pressure Data

Outputs from the dynamic pressure transducers were recorded on magnetic tape. The transducer data were processed into 1.25-Hz narrow-band spectra with a spectrum analyzer.

Procedure

Preliminary Model Sizing Tests

The desired flow conditions in the model at high tailpipe-to-ambient pressure ratios were 0.3 tailpipe Mach number M_5, 0.3 offtake duct Mach number M_d, offtake flow w_d 45% of tailpipe flow w_5, and ventral flow w_v 10% of w_5.

The model size was based on a 13.5-in.-diam tailpipe from a previous test program. The offtake duct was the diameter of commercial pipe that was closest to the size estimated to give all the desired flow conditions, assuming choked nozzle flows and $1.0q_5$ pressure loss in the offtake ducts, where q_5 is the tailpipe dynamic pressure. The estimate of pressure loss came from experience with ventral nozzles,[3] but it turned out to be too low as shown later in this article. Because of the many uncertainties, the offtake flow control and ventral nozzles were sized in trial-and-error preliminary experiments. At first the three nozzles were purposely undersized. A performance test was run to measure duct Mach numbers and flow rates. The resulting data were extrapolated to choose larger nozzle areas. The larger nozzles were machined to the new required geometric shapes. This process was repeated to set the final nozzle sizes. The final nozzle sizes were 7.10 in. (39.6 in.^{2}) for each offtake nozzle and 3.21 in. (8.09 in.^{2}) for the ventral nozzle.

Performance Tests

Performance testing consisted of measuring the internal flow conditions over a range of tailpipe total-to-ambient pressure ratios PR_5, up to 5.0. For each PR_5, mass flow rates (actual and ideal), Mach numbers, and area-averaged total pressure at the various model stations were computed.

Flow Pattern Tests

Flow pattern tests were done with the final-sized nozzles. A traverse of an offtake inlet (station 5A2) on the horizontal diameter was made with the calibrated flow angle probe at $PR_5 = 4.5$. The stream flow conditions were calculated from the same data using an iterative procedure.

Flow visualization paint streaks were made by placing small dabs of thick oily paint in a regular pattern on the inside surface of the model. Airflow was started quickly, held for approximately 1 min, and shut off. The paint ran along flow streamlines, and the resulting streaks were photographed for record.

Results and Discussion

Performance

This section presents and discusses flow, Mach number, and pressure loss results for the model with two preliminary and the final nozzle sizes at PR_5 up to 5. In addition, the total pressure distributions at the tailpipe, ventral nozzle, and offtake stations are shown for $PR_5 = 4.5$.

Airflow

The tailpipe flow rate w_5 was measured by facility equipment, and the offtake and ventral flow rates were measured by nozzles on the model. All the flow rates were constant after the offtake nozzles choked. The measured w_5 was slightly less than the sum of the nozzle flows. The difference was as much as $-0.022w_5$ at the highest PR_5. Ventral nozzle flow inaccuracy is not known, but is estimated to be $\pm 2\%$ because of the distorted total pressure at the nozzle inlet.

Offtake Ducts

The performance of the offtake ducts measured in the two preliminary and the final nozzle sizing tests described in a preceding section is shown in Fig. 4. For each nozzle area, the pressure loss and the Mach number at the end of the offtake duct, station 5C, increased with the tailpipe pressure ratio and became nearly constant after the nozzles choked. This behavior is not unusual, although the magnitude of the pressure loss, up to 15.5% of the tailpipe pressure, is much greater than the 1.5% loss reported in tests of elbows with uniform inflow.[9] Although not shown in Fig. 4, the pressure loss was the same in each offtake within 0.2% of the tailpipe pressure. The flow split, as a percentage of tailpipe flow, was satisfactorily close to the desired value.

The performance of the model with the ventral nozzle closed is also shown in Fig. 4. In comparison to the same configuration with the ventral nozzle open, the tailpipe Mach number

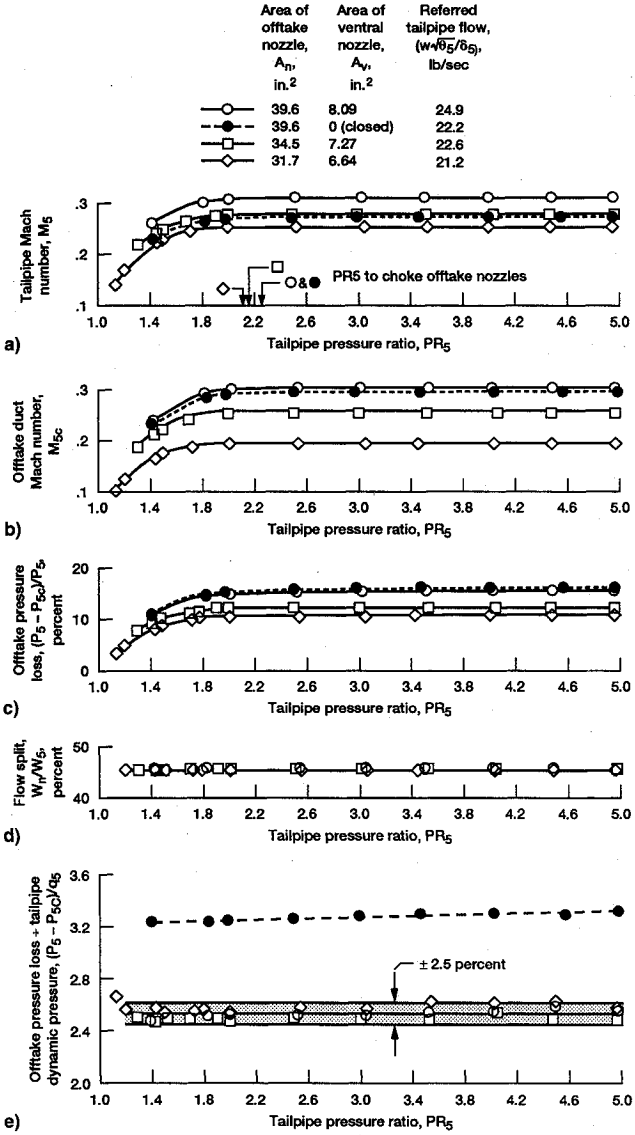

Fig. 4 Offtake system performance: a) tailpipe Mach number, b) Mach number near end of offtake duct, c) offtake pressure loss, d) flow split, and e) total pressure loss related to tailpipe dynamic pressure.

decreased because of reduced total flow, but the offtake Mach number, pressure loss, and flow rate were about the same.

The offtake pressure loss expressed in terms of tailpipe dynamic pressure q_5 is shown in Fig. 4e. With the ventral open all the loss data fell within a band centered at $2.53q_5$ (in contrast to $0.25q_5$ for uniform inflow[9]). With the ventral nozzle closed the tailpipe Mach number and dynamic pressure were less, and the pressure loss band increased numerically to $3.25q_5$. This result implies that the turning loss for a given geometry is dependent mainly on the offtake flow rather than some tailpipe parameter such as Mach number. However, more data are needed to trust such a generalization.

Ventral Duct

The ventral duct performance trends were the same as measured for the offtake ducts. The final-sized ventral nozzle became choked at $PR_5 = 2.1$, and the pressure loss from station 5 to station V was 8.4% of the tailpipe pressure. All the pressure loss data fell in a relatively narrow band centered at $1.35q_5$.

Total Pressure Distribution

The total pressures measured at various stations in the model are shown in Fig. 5 for $PR_5 = 4.5$. The contour plots at stations 5B and 5C were made by combining the data from two test readings, one with the rakes positioned as shown in Fig. 3, the other with the same rakes rotated 45 deg in the measuring plane. Because of geometric and flow similarities, these results are applicable to either offtake.

The tailpipe inflow at station 5 (Fig. 5a) had a thin boundary layer and uniform total pressure in the core. The boundary layer was presumed to be turbulent because of the boundary-layer trip located approximately one tailpipe diameter ahead of station 5 (Fig. 2 and Ref. 10).

At the elbow exit (station 5B), the highest total pressure was measured near the outside wall. The total pressure fell to lower values near the center of the duct, then increased again near the inside wall. Using wall pressures shown in a subsequent figure, the calculated Mach number was approximately 0.5 at the outside wall and 0.35 at the inside wall. The flow then diffused as it traveled down the duct, and the total pressure distortion became much less at station 5C, the end of the duct and entrance to the offtake nozzle.

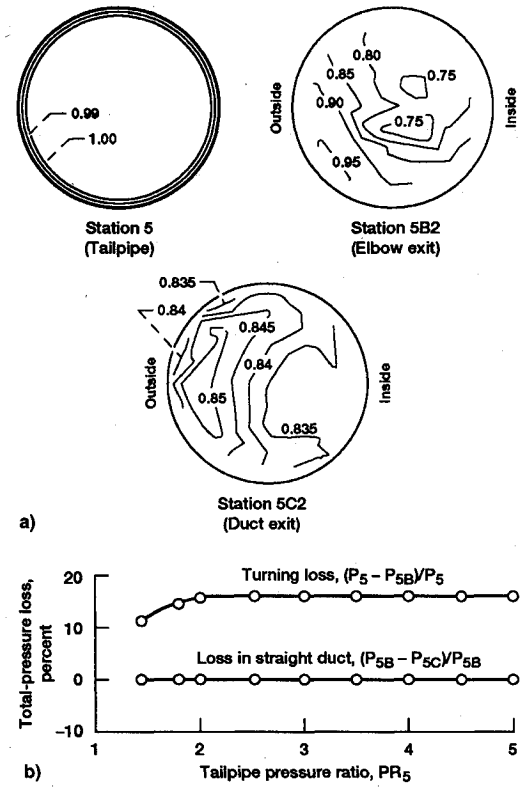

Fig. 5 Offtake total pressure. Final nozzle sizes: a) total-pressure contour plots at $PR_5 = 4.5$. Numbers show contour level ratioed to P_5. Plots shown looking into flow and b) pressure loss distribution.

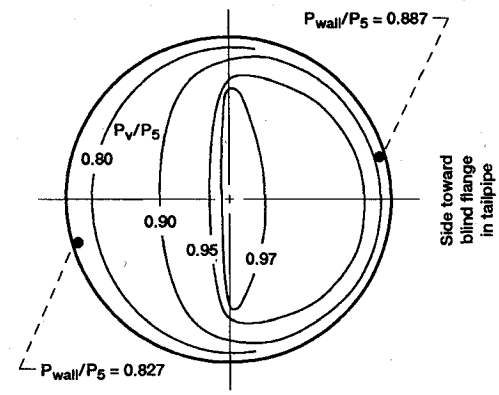

Fig. 6 Total-pressure contours at station V (ventral nozzle inlet) estimated from rake data; $PR_5 = 4.5$.

The distribution of the offtake total pressure loss is given in Fig. 5b. Nearly all the loss occurred as the flow turned from the tailpipe station 5 into and through the elbow to station 5B. The loss in the straight duct from station 5B to station 5C was very small.

The total pressure contours at the ventral nozzle inlet are shown in Fig. 6. The contours were estimated from the rake pressure data. Pressure and flow were strongest in the aft part of the ventral duct because flow separated from the front edge and could not diffuse and mix completely in the short duct. Reverse flow probably occurred near the front wall because the measured wall static pressure was greater than the nearby rake total pressures.

Wall Pressures

The wall pressures measured at taps located throughout the model are reported in this section as ratios of the tailpipe total pressure P_5 at $PR_5 = 4.5$. Data are given for both the ventral-nozzle-open and ventral-nozzle-closed cases. These wall pressures can aid in understanding flow behavior in the tailpipe and offtakes.

Tailpipe

The tailpipe wall pressure distribution is shown in Fig. 7. Pressures were somewhat higher for the ventral-nozzle-closed case, mostly because the total flow and Mach number decreased. Side-to-side differences were small, consistent with flow equality in the offtakes. Specifically, pressures were lowest near the offtake openings. Further aft in the tailpipe the wall pressures, including the blind flange, were less than station 5 total pressure. The decrement at the blind flange probably represents diffusion loss of the air that flowed into the tailpipe aft of the offtake openings. For total pressure equal to blind flange pressure, the Mach number in the closed end of the tailpipe was about 0.05. The pressure differences top-to-bottom in the tailpipe (Fig. 7b) were similar to those side-to-side except near the ventral opening.

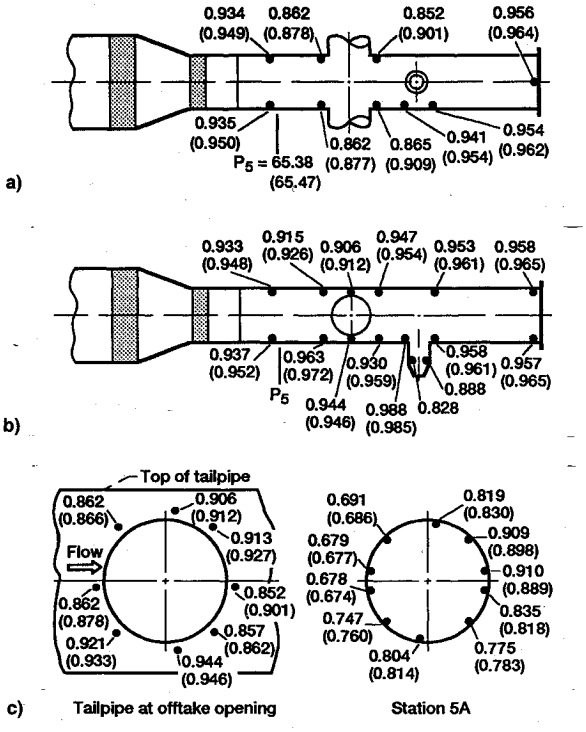

Fig. 7 Tailpipe wall pressure divided by station 5 total pressure (p_w/P_5) at $PR_5 = 4.5$. Upper numbers are for open ventral nozzle, numbers in parentheses are for closed ventral nozzle: a) horizontal section, top view; b) vertical section, side view; and c) offtake opening, looking from tailpipe into opening.

Pressures measured on the tailpipe wall around the offtake opening and in the offtake duct just downstream of the opening (station 5A) are given in Fig. 7c. The highest pressures always occurred in the upper right quadrant. The lowest pressures occurred at the front edge of the opening, showing that velocity probably was highest there. The figure shows that pressures on the tailpipe wall were generally higher than wall pressures corresponding radially at station 5A. These pressure differences tended to drive flow locally into the offtake.

Offtakes

Wall pressures measured in an offtake elbow and duct are shown in Fig. 8. Just downstream of the offtake opening, the pressures were always greater on the outer wall than on the inner wall, indicating that the flow was always turning as it moved through the elbow and the first part of the long straight duct. The highest pressure was $0.87P_5$, so cooling the offtake elbows and ducts with bypass air in a turbofan installation would be feasible. At the end of the duct the pressure was the same all around the wall, consistent with the previous observation that the flow diffused through the duct and became more nearly uniform at the offtake nozzle entrance. There is no indication from the measured pressures that the flow was choked anywhere in the system ahead of the nozzles.

Dynamic Pressures

Dynamic pressures at the offtake openings and at the center of the blind flange were measured with high-frequency-response transducers (Fig. 3). Spectra from a transducer at an offtake opening (Fig. 9a) show some periodic activity between 15–35 Hz. However, the spikes result in only about a 0.01 Mach number change in flow velocity, which does not seem to represent a significant flow oscillation.

A standing wave in the closed end of the tailpipe would produce maximum pressure variations at the blind flange. The quarter-wave-length frequency is between 64–80 Hz for waves originating at the offtake opening. The spectra from the transducer at the blind flange (Fig. 9b) do not show spikes near these frequencies, so this type of resonance was not present.

Flow Patterns

The stream flow pattern entering an offtake opening was measured with a calibrated flow angle probe at $PR_5 = 4.5$. Wall flow patterns in and around the offtake entrance were

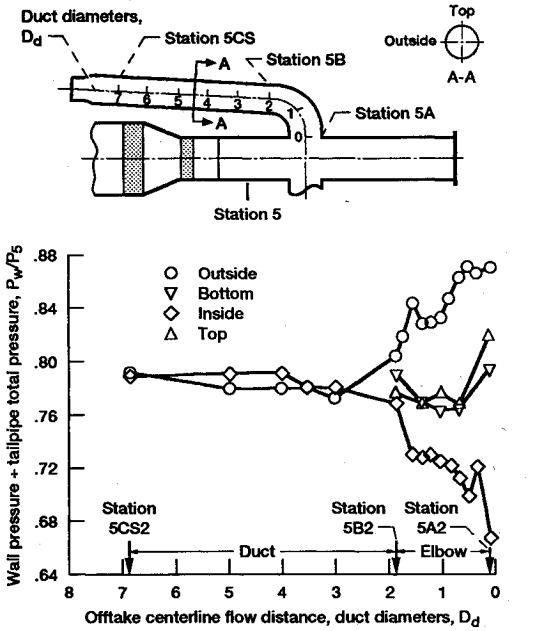

Fig. 8 Offtake wall pressure for $PR_5 = 4.5$; ventral open. Results applicable to either offtake side.

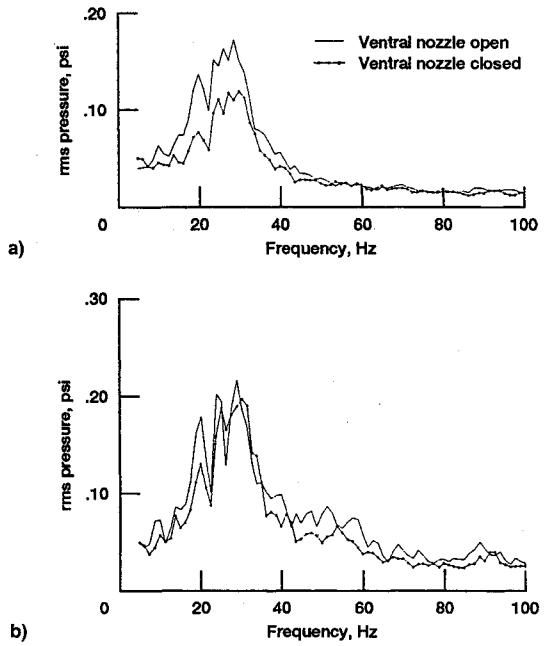

Fig. 9 Dynamic wall pressure. Spectral bandwidth, 1.25 Hz: a) offtake, side 2 and b) center of blind flange.

obtained from flow visualization paint streaks. The flow patterns complement the pressure data and contour plots given in previous figures.

Offtake Opening Traverse

Results of the flow angle probe traverse at the side 2 elbow entrance (station 5A2) are shown in Fig. 10 for the ventral nozzle both open and closed. The traverses were made on the horizontal centerline and started at the aft edge of the opening.

The total pressure ratio is the ratio of the computed probe total pressure to the station 5 total pressure. For the ventral-nozzle-open case the pressure was generally high in the aft and central parts of the opening; in fact, the pressure showed little or no loss from station 5 over part of the traverse path. When the ventral nozzle was closed, the pressure dipped to a much lower level about 3.5 in. from the aft edge, but otherwise was similar to the traverse with the ventral nozzle open. This change in total pressure distribution hints that much of the offtake inflow pattern changed with the ventral nozzle closed, but the pressure loss from station 5 to station 5C was the same whether the ventral nozzle was open or closed (Fig. 4). No explanation is known for this unusual result.

The Mach number computed from the traverse data was about 0.4 in the aft part of the opening, and gradually increased with traverse distance to a peak value of 0.73. These results, plus the total pressure data, reveal that the stream static pressure decreased along the traverse path. The Mach number fell off rapidly in the turning flow near the front edge of the opening.

The angles at which the flow entered the offtake opening are called herein the approach angle (measured in the horizontal plane) and the swirl angle (measured in the vertical plane). Flow generally approached the opening at angles between 40–65 deg, and up to 70 deg (more nearly normal to the tailpipe wall) at the aft and front edges. Flow swirled downward in the aft part of the opening, then in the opposite direction at the central part. The swirl disappeared near the front edge. The approach and swirl angles were similar for both the ventral-nozzle-open and ventral-nozzle-closed cases.

Flow Visualization

The photographs in Fig. 11 show flow visualization streaks drawn on a scale mockup of the model. The mockup tailpipe

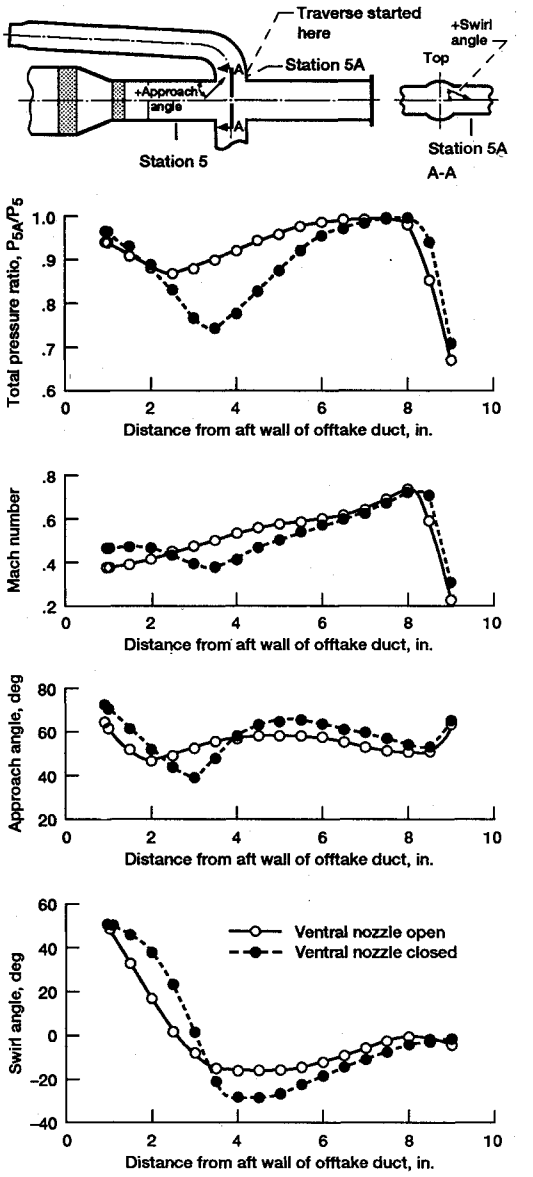

Fig. 10 Flow conditions on offtake horizontal centerline at elbow entrance (station 5A2) for $PR_5 = 4.5$: a) total pressure ratio, b) Mach number, c) approach angle, and d) swirl angle.

was split on the (vertical) plane of symmetry, and the mockup elbow on side 2 could be opened to show the inner wall.

Figure 11a shows streaks on the tailpipe wall. The inflow streaks at station 5 were axial in direction, and the flow was uniform (Fig. 5a). Streaks around the opening show that flow entered radially around most of the periphery as expected from the pressure differentials given in Fig. 7c. In addition, much of the flow impacted the aft duct wall just inside the offtake opening near station 5A, then followed the elbow wall downstream. Some of this flow, in the upper right quadrant, spilled back into the tailpipe and swirled in a clockwise direction to re-enter the tailpipe in the lower right and bottom quadrants. This is the same swirl measured with the flow angle probe (Fig. 10). Further back in the tailpipe, streaks show that flow entering the ventral duct probably separated at the front of the opening as in other ventral nozzle tests,[3] and impacted the aft wall of that duct (Fig. 6). The streaks indicate that all the ventral flow entered the duct from the front side, but they do not tell whether the flow came from the central or wall regions of the tailpipe. Still further aft in the tailpipe, streaks show that the flow continued to move toward the blind flange, but some of the streaks suggest that it broke into complex three-dimensional swirling flows. In any case, by

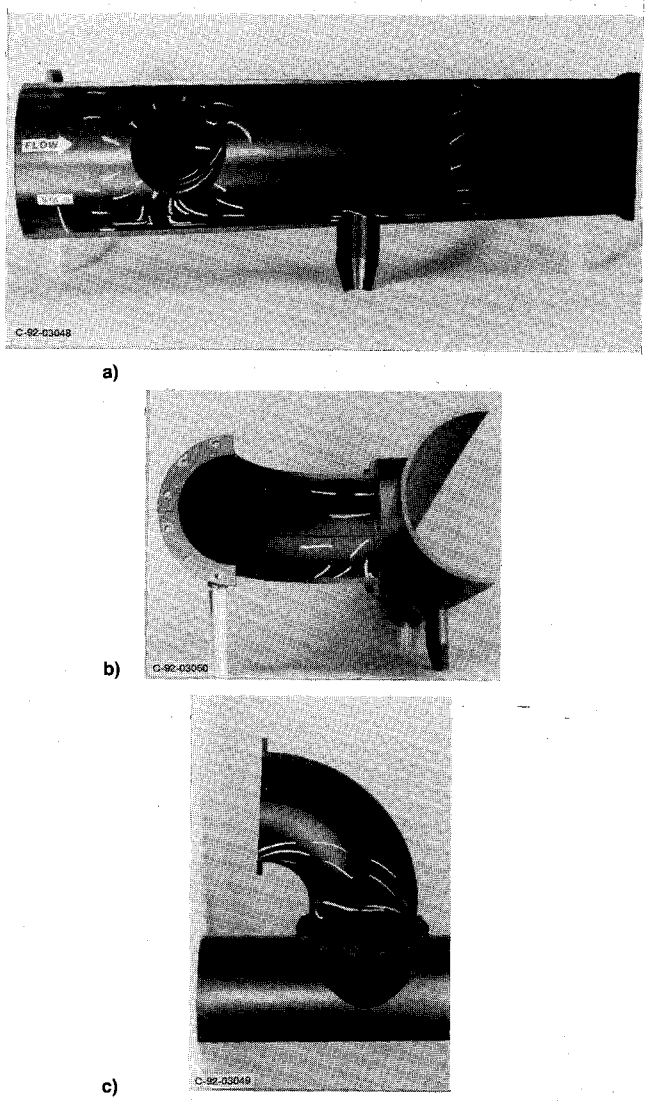

Fig. 11 Flow visualization streaks on scale mockup of model: a) tailpipe cut at plane of symmetry, b) inside wall of elbow removed, and c) top wall of elbow removed.

continuity there must have been flow in the reverse direction elsewhere in the tailpipe.

In Figs. 11b and 11c, parts of the elbow have been removed to show streaks inside the elbow. As stated previously, much of the flow that impacted the aft wall of the opening flowed downstream along the elbow wall. Streaks illustrating this flow can be seen in Fig. 11b. In addition, some of the flow ran along the lower wall of the elbow, as shown in Fig. 11c, and joined with the swirling flow entering from the tailpipe. This combined flow moved across the wall toward the elbow exit, without following the wall curvature. The net result was a flow swirling in a clockwise direction through the elbow (looking downstream). The swirl probably aided mixing and diffusion in the long offtake duct, and thus contributed to the more uniform total pressure measured at the duct exit (Fig. 5a).

Conclusions

A generic one-third scale model of a tailpipe offtake system for an ASTOVL aircraft was tested at the NASA Lewis Powered Lift Facility. The flow split was 45% to each of two offtakes and 10% to a small ventral nozzle. Offtake flow turned through a total of 177 deg. The tests were performed with unheated air over a range of tailpipe-to-ambient pressure ratios up to 5. Important test results when the offtake flow control nozzles were choked are as follows:

1) Pressure loss in the offtake ducting was 15.5% of the tailpipe total pressure (2.5 times dynamic pressure) at a tailpipe Mach number of 0.31. The loss did not change when the ventral nozzle was closed off, although the tailpipe Mach number decreased to 0.27 and the flow pattern into the offtake opening was changed.

2) Most of the pressure loss occurred in turning flow into and through the offtake elbows. Flow patterns at the offtake openings were complex. Measurements showed large total pressure distortion and high stream Mach number in this flow. The flow diffused in a swirling manner in the long straight offtake ducts and became much more uniform at the end of the ducts.

3) No significant periodic pressure fluctuations were measured at the offtake openings or at the blocked end of the tailpipe.

4) Wall pressures throughout the tailpipe were less than 96% of tailpipe total pressure, and in the offtake ducting were less than 88%.

5) The ventral duct pressure loss was 8.4% of the tailpipe total pressure. The flow was concentrated in the aft part of the ventral duct, and total pressure distortion was large at the ventral nozzle inlet.

In application to flight hardware design, these tests showed that turning aids in the offtakes, such as rounded entrances or guide vanes, are needed to reduce pressure loss. Guide vanes may have to be tailored to match flow approach angles at the offtake openings. Larger offtakes, noncircular openings such as elliptical shapes, or convergent elbows may also reduce loss. Offtake ducts should be long to promote mixing and reduce distortion. Wall pressures in the offtake system are low enough that turbofan bypass air probably could be used for duct cooling. A small amount of ventral or tailpipe throughflow may not affect pressure loss in the offtake system. Additional model testing also could show the effects of core/bypass flow mixing, the effects of offtake shutoff valve characteristics on performance during transition between hover and horizontal flight, and provide applicable data to assist CFD prediction of viscous flow losses.

Acknowledgments

The CFD analysis was done by J. Rhodes at McDonnell-Douglas Aerospace. The experimental work was performed by B. Esker, G. Perusek, and B. Dastoli at NASA Lewis Research Center.

References

[1]Wynosky, T. A., and Szyszko, C. J., "V/STOL Deflector Aerodynamic Design Criteria," AIAA Paper 73-1181, Nov. 1973.

[2]Cooper, G. K., and Sirbaugh, J., "The PARC Distinction: A Practical Flow Simulator," AIAA Paper 90-2002, July 1990.

[3]McArdle, J. G., and Smith, C. F., "Experimental and Analytical Study of Close-Coupled Ventral Nozzles for ASTOVL Aircraft," NASA TM-103170, July 1990.

[4]Smith, C. F., and McArdle, J. G., "Analysis of Internal Flow in a Ventral Nozzle for STOVL Aircraft," AIAA Paper 90-1899, July 1990.

[5]Rhodes, J. A., Esker, B. S., and Smith, C. F., "Computational and Experimental Investigation of Subsonic Internal Reversing Flows," AIAA Paper 92-3791, July 1992.

[6]Bean, H. S., (ed.), *Fluid Meters—Their Theory and Application*, 6th ed., American Society of Mechanical Engineers, New York, 1971.

[7]Krause, L. N., and Dudzinski, T. J., "Flow-Direction Measurement with Fixed-Position Probes in Subsonic Flow over a Range of Reynolds Numbers," NASA TM-X-1904, May 1969.

[8]Stitt, L. E., "Exhaust Nozzles for Propulsion Systems with Emphasis on Supersonic Cruise Aircraft," NASA RP-1235, May 1990.

[9]Higginbotham, J. T., Wood, C. C., and Valentine, E. F., "A Study of the High-Speed Performance Characteristics of 90° Bends in Circular Ducts," NACA TN-3696, June 1956.

[10]Raman, G., Zaman, K. B. M. Q., and Rice, E. J., "Initial Turbulence Effect on Jet Evolution with and Without Tonal Excitation," AIAA Paper 87-2725, Oct. 1987.